Environmental Research 159 (2017) 579–587

Contents lists available at ScienceDirect

Environmental Research

journal homepage: www.elsevier.com/locate/envres

Cytotoxic effects of commonly used nanomaterials and microplastics on cerebral and epithelial human cells

Gabriella F. Schirinzi[a,d], Ignacio Pérez-Pomeda[b,d], Josep Sanchís[a,d], Cesare Rossini[c,d], Marinella Farré[a,d,*], Damià Barceló[a,b,d]

[a] Institute of Environmental Assessment and Water Research (IDAEA-CSIC), Barcelona, Catalonia, Spain
[b] Institute for Advanced Chemistry of Catalonia (IQAC), Barcelona, Catalonia, Spain
[c] Thermo Fisher Scientific, StradaRivoltana, 20090 Rodano, Milano, Italy
[d] Catalan Institute for Water Research (ICRA), Girona, Catalonia, Spain

ARTICLE INFO

Keywords:
Nanomaterials
Microplastics-nanoplastics
Cytotoxicity
ROS effect

ABSTRACT

Plastic wastes are among the major inputs of detritus into aquatic ecosystems. Also, during recent years the increasing use of new materials such as nanomaterials (NMs) in industrial and household applications has contributed to the complexity of waste mixtures in aquatic systems. The current effects and the synergism and antagonisms of mixtures of microplastics (MPLs), NMs and organic compounds on the environment and in human health have, to date, not been well understood but instead they are a cause for general concern.

The aim of this work is to contribute to a better understanding of the cytotoxicity of NMs and microplastics/nanoplastics (MPLs/NPLs), at cell level in terms of oxidative stress (evaluating Reactive Oxygen Species effect) and cell viability. Firstly, the individual cytotoxicity of metal nanoparticles (NPs) (AgNPs and AuNPs), of metal oxide NPs (ZrO_2NPs, CeO_2NPs, TiO_2NPs, and Al_2O_3NPs), carbon nanomaterials (C_{60}fullerene, graphene), and MPLs of polyethylene (PE) and polystyrene (PS) has been evaluated *in vitro*. Two different cellular lines T98G and HeLa, cerebral and epithelial human cells, respectively, were employed. The cells were exposed during 24–48 h to different levels of contaminants, from 10 ng/mL to 10 μg/mL, under the same conditions. Secondly, the synergistic and antagonistic relationships between fullerenes and other organic contaminants, including an organophosphate insecticide (malathion), a surfactant (sodium dodecylbenzenesulfonate) and a plasticiser (diethyl phthalate) were assessed. The obtained results confirm that oxidative stress is one of the mechanisms of cytotoxicity at cell level, as has been observed for both cell lines and contributes to the current knowledge of the effects of NMs and MPLs-NPLs.

1. Introduction

During the last century, technological developments triggered the promotion of new materials such as plastics which, due to their excellent mechanical properties, versatility and low cost impelled their consumption. Therefore, since the 1940s, when the first production of plastics at the industrial scale took place, their manufacture has steadily grown (Al-Salem et al., 2010). In addition, from 2000 to 2010 a massive growth of the world's yearly consumption was produced in relation to the growing demand in developed economies such as the EU, Canada and the USA, together with the new demand and enhanced consumerism in emerging economies such as China. However, this expansion comes with the generation of tonnes of waste, some of which are non-biodegradable and toxic by-products, resulting in new undesirable impacts on the environment (Tongesayi and Tongesayi, 2016). Moreover, to date, the environmental fate and time of total degradation have not been well understood. In particular, microplastics (MPLs), defined as small particles at the millimetre to sub-millimetre size range with high densities, are a new environmental risk (da Costa et al., 2017; Horton et al., 2016). The origin of MPLs can be from the manufacturing of micro-beads that are used in cosmetic facial cleansers (Fendall and Sewell, 2009). Alternatively, secondary MPLs can result from the fragmentation and erosion of plastic items (Aueviriyavit et al., 2014). During recent years, the presence of plastics and MPLs in marine and coastal areas has been a cause for concern (Cole et al., 2011), attracting the attention of both researchers and the general public. Low density MPLs contaminate the sea surface and due to their small size, which is similar to plankton, they could be introduced into the food chain (Wright et al., 2013). Another important uncertainty is whether these compounds can act as vector for transferring pollutants to biota,

* Corresponding author at: Institute of Environmental Assessment and Water Research (IDAEA-CSIC), Barcelona, Catalonia, Spain.
E-mail address: mfuqam@cid.csic.es (M. Farré).

http://dx.doi.org/10.1016/j.envres.2017.08.043
Received 2 June 2017; Received in revised form 23 August 2017; Accepted 23 August 2017
Available online 11 September 2017
0013-9351/

thus leading to their bioaccumulation (Llorca et al., 2014; Cedervall et al., 2012).

On the other hand, during the last decade, developing nanotechnology has promoted a new series of materials and opportunities for different industrial and consumer products. Nanomaterials (NMs) are characterized by their dimensions in the range of 1–100 nm. Key factors driving the fact that NMs differ significantly from pollutants at the macro-scale are their high surface area and quantum effects (Farré and Barceló, 2012). These factors can modify some properties such as electrical or optical reactivity and strength, thereby altering the fundamental physical and chemical properties of conventional materials. Current applications in nanotechnology span from electronics (Sanchez et al., 2011), household products, food additives and food packaging (Eleftheriadou et al., 2017; Ranjan et al., 2014), personal care products, nanomedicine (Marchesan and Prato, 2013), sports equipment, textiles (Contado, 2015), among many others. With the ongoing commercialization of NMs, human exposure to nanoparticles will dramatically increase, and evaluation of their potential toxicity is essential (Holden et al., 2016).

During recent years, a high number of studies have evaluated the ecotoxicological effects on NMs (Yan et al., 2011; Fu et al., 2014) as well as the environmental fate and behaviour of NPs (Nickel et al., 2014). In particular, NMs and NPs, which currently have an extensive range of applications such as metal and metal oxide NPs (among which there are silver nanoparticles (AgNPs), gold nanoparticles (AuNPs), and titanium dioxide nanoparticles (TiO_2), and more) have been studied more by using *in vivo* and *in vitro* approaches (Johnston et al., 2010; Wijnhoven et al., 2009). For instance, due to the antibacterial properties of AgNPs, they are exploited in an increasing number of consumer and medical products such as packaging materials (Aueviriyavit et al., 2014), clothing, wound dressings, deodorants and spray rooms (Vigneshwaran et al., 2007; Lee et al., 2007). Regarding Au-NPs, they are used in current biomedical applications including diagnostics, photo-thermal and photodynamic therapies and delivery of target molecules such as drugs or peptides (Austin et al., 2015; Dykman and Khlebtsov, 2012). On the other hand, recent research has investigated the uptake in plants of some metal oxide NPs such as $nCeO_2$ (nano-scaled cerium oxide) and the introduction of these into the food chain (Rico et al., 2011). On the other hand, other NMs such as fullerenes and carbon nanotubes (CNTs) have recently been considered in different toxicological and bioaccumulation studies (Maes et al., 2014) because, firstly, in addition to nanotechnology they can be emitted by incidental and natural sources into the environment. Secondly, because of their adsorption/desorption capabilities, they could influence the toxicity of other co-contaminants (Sanchís et al., 2016).

The lack of information on the toxicology of NMs under certain scenarios of exposure has led to the restricted use of some of them for certain applications that are directly in contact with humans, such as inclusion in cosmetics, detergents and food, in the prevention of their potential toxicity or long-term secondary adverse effects (Yoo-Iam et al., 2014; Khanna et al., 2015). But, due to the impact of anthropogenic activities, the concentrations of some NPs in the aquatic environment increase and organisms can uptake them by ingestion or through the skin. Therefore, the increasing bioconcentration of these substances in the tissue of organisms leads to successively higher levels that move along the food chain. However, this field continues being in an initial phase of development and most of the current data are regarding high concentrations of exposure and the effects of NPs and NMs at low concentrations of exposure in complex mixtures that, to date, have not been well understood (Holden et al., 2016).

The aim of this study is to contribute to the better understanding of toxicity of NMs including AgNPs, AuNPs, ZrO_2NPs, CeO_2NPs, TiO_2NPs, Al_2O_3NPs, C_{60} fullerene, graphene, and MPLs (polyethylene and polystyrene) at cell level in terms of oxidative stress and cell viability. The cytotoxic responses of two different cell lines T98G and HeLa, cerebral and epithelial human cells, respectively, that were exposed to the same conditions, were evaluated. Moreover, the synergistic and antagonistic relationships between fullerenes and other organic contaminants, an organophosphate insecticide (malathion), a surfactant (sodium dodecylbenzenesulfonate) and a plasticizer (diethyl phthalate) were assessed. The selection of these three organic compounds was based on their use, their presence and their toxicity in the aquatic environment, as well as their physicochemical properties. Malathion is a commonly used insecticide and in different studies has been related with oxidative stress induction. Sodium dodecylbenzenesulfonate is a commonly detected surfactant in rivers and coastal waters. Furthermore, diethyl phthalate is a widely used plasticizer.

Most of the reported works have explored the cytotoxicity at much higher concentrations in relation to, for example, their applications as drug carriers or nanomedicine. Here, we consider much lower levels, such as those that can be considered by incidental exposure. Notwithstanding, in the case of MPLs almost no data have been reported to date.

2. Materials and methods

2.1. Chemicals

To the best of our knowledge, the standards and mediums used in this study were of the highest purity available. Dulbecco Modified Eagle's Media (DMEM) and trypsin-EDTA were supplied by Sigma-Aldrich. Fetal Bovine Serum (FBS) and Penicillin/Streptomycin Solution were obtained from Invitrogen™ (Thermo-Fisher Scientific). Dulbecco's phosphate-buffered saline (PBS), dimethyl sulfoxide (DMSO), Hoechst 33258 (bisBenzimide H 33258 ≥ 98%) and dihydroethidium (DHE) (≥ 95%) were purchased from Merck Millipore (Darmstadt, Germany). Salts and analytical standards silver nitrate (ACS reagent, ≥ 99%), trisodium citrate (≥ 98%), gold nanoparticles (10 nm particles size, stabilised suspension in 0.1 mM PBS), zirconium (IV) oxide (suspension 10% wt in H_2O, < 100 nm particles size), cerium (IV) oxide (suspension 10% wt in H_2O, < 25 nm particles size), titanium (IV) oxide (~21 nm particles size, ≥ 99.5% trace metals basis), fullerene-C_{60}, fullerol and fullerene soot (76% of C_{60} fullerene, 22% of C_{70} fullerene and 2% of higher-order fullerenes) produced by the Krätschmer – Huffman method (Kratschmer et al., 1990) was purchased from Sigma-Aldrich (Steinheim, Germany). Aluminium oxide 90 active neutral (0.063–0.200 mm particle size) was purchased from Merck Millipore (Darmstadt, Germany). Graphene nano-powder consisting of 1.5–10 μm particles (4.5 μm mean size) composed of 12 nm graphene flakes (equivalent to 30–50 graphene layers) was supplied by Graphene Supermarket (Reading, MA, USA). The organic compounds used, such as malathion (≥ 99%), diethyl phthalate PESTANAL® (DEHP) (≥ 99.5%) and sodium dodecylbenzenesulfonate (C_{12}-LAS) (~80%), were purchased from Sigma-Aldrich.

Silver nanoparticles (AgNPs) were synthetized using trisodium citrate as a reducing agent (Rashid et al., 2013). In brief, all solutions of reacting materials were prepared in HPLC water. Fifty (50) mL of 0.001 M $AgNO_3$ was heated to its boiling point and then 5 mL of 1% trisodium citrate was added, drop by drop. The solutions were heated and stirred vigorously until there was a change of color to pale yellow. Then, the obtained suspension was allowed to reach room temperature. The silver colloid suspension was characterized by nanoparticle tracking analysis (NTA) using a NanoSight LM10 (NanoSight Ltd., Salisbury, UK). This technique allows visualizing particles in liquids, relating Brownian motion and particle size. For this characterization, measurements were carried out in static mode. To adjust camera level and threshold, a pre-scan was carried out.

Polyethylene (PE) microspheres (3–16 μm) accompanied by NPs with sizes between 100 and 600 nm were purchased from Cospheric LLC (Santa Barbara, CA, USA) and polystyrene (PS) (10 μm, 1% solids) accompanied by NP with sizes between 40 and 250 nm were obtained from PolySpherex™ Polystyrene microspheres which are purchased

from Phosphorex (Hopkinton, MA, USA). The presence of NPs in each case was validated by NTA (see Fig. S1 of Supporting Information section). The cell lines employed in these experiments were human glioblastomamultiforme T98G cells and human cervical carcinoma HeLa cells that were kindly provided by Dr. Gemma Fabriàs from the Institute for Advanced Chemistry of Catalonia (IQAC-CSIC).

2.2. Standard suspension and solutions

Dry powder of metal oxide NPs (ZrO_2, TiO_2, CeO_2, Al_2O_3), metal NP (Au and Ag), fullerol, and MPLs of PE and PS microspheres were weighed and diluted in PBS in order to obtain a mother solution of 100 mg/L and then with the cellular medium DMEM. While AuNPs and AgNPs were diluted from stable suspensions. Mother solutions were subsequently diluted in the assay range of 50 μg/L to 1–10 mg/L.

2.3. Carbon NMs dispersion procedure

Fullerenes (C_{60} 76%, C_{70} 22%, with the remainder being higher-order fullerenes) and graphene standard had been aged during 40 d in mesocosms, simulating the aging of materials under real estuary conditions with controlled salinity, pH and organic matter content (Sanchís et al., 2015). The use of artificial dispersing agents as solvents was avoided in order to reproduce relevant environmental conditions (Fig. S2). Mother solutions were subsequently diluted in the assay range of 50 μg/L to 10 mg/L.

2.4. Binary mixture

Binary mixtures containing fullerene soot and organic contaminant were prepared at different concentration ratios. In each experiment, increasing concentrations of organic contaminants (0 − 60 mg/L) were tested in triplicate. Each series was prepared with a constant concentration of fullerene soot suspension 0, 1.0 and 5.0 mg/L.

2.5. Cell culture

The cell lines employed in this experiment were T98G and HeLa cells, which are both human cells that are commonly used in research. Both cell lines were grown in cell culture flasks containing DMEM supplemented with 10% FBS and 1% antibiotics (100 U/mL penicillin and 100 μg/mL streptomycin). The cells were incubated at 37 °C in a humidified incubator set at 5% CO_2. Cells were subcultured according to standard cell culture protocols prior to cytotoxicity assays.

2.6. In vitro cytotoxicity assay

T98G and HeLa cells were seeded in 96-well plates at 25,000 cells/well. After 24 h, the medium was removed and cells were exposed for 24–48 h to the different NMs, polymers and mixtures at concentrations from 10 ng/mL to 10 μg/mL. At the end of exposure, the tested solutions were removed and the cells were stained with two fluorescent biomarkers for 30 min at 37 °C in a 5% CO_2 atmosphere. Fluorescent biomarkers were (1) 2-[2-(4-hydroxyphenyl) − 6-benzimidazolel-6-(l-methyl-4-piperazyl)-benzimidazole trihydrochloride (Hoechst 33258), which is a fluorescent compound that interacts with DNA (Excitation/Emission maxima = 352/461 nm). A 10 μM Hoechst 33258 solution was used as an indicator of cell viability, and (2) DHE solution 25 μM was used as a superoxide ($O_2^{\cdot-}$) generation indicator.

Then, the labeling solutions were aspirated and cells were rinsed with PBS. Fluorescence measures were determined at 485 nm (Hoechst) and 549 nm (DHE) emission wavelengths using CellInsight™ NXT High Content Screening (HCS) Platform (Thermo Scientific).

However, DHE is a colourless compound but it is cell-permeable. If there is the presence of superoxide anion ($O_2^{\cdot-}$) in the cytoplasm, DHE is oxidated to ethidium which intercalates into the DNA in the nucleus and fluoresces red color (Excitation/Emission maxima = 510/595 nm).

2.7. High-content analysis

The cell viability and the oxidative stress were measured via High-Content Analysis (HCA). This technique combines automated microscopy and cell fluorescence-tagging with Hoechst 33258 and DHE. The acquisition was performed with a 10 × lens using two channels with two different wavelengths (λ_1 = 485 nm and λ_2 = 549 nm) that are close to the Hoechst and DHE emission maximum, respectively. Optics focus and acquisition brightness were optimized. The obtained micrograph is a result of a magnified image of the well, which permits to recognise automatically the cells stained with fluorescent compound. Primary objects were validated or rejected according to the following criteria: emplacement in the micrograph, shape, area and light intensity; see Fig. S3 of Supporting information section on the micrograph of T98G cells.

2.8. Statistics

The data were expressed as mean ± SD of three independent experiments. Wherever appropriate, the data were subjected to statistical analysis using a one-way analysis of variance (ANOVA) test, followed by Dunnett's test to compare all data with the control values. A value of $P < 0.05$ was considered to be statistically significant only for a high concentration of contaminant. GraphPad 4.0 Software was used for the statistical analysis.

3. Results and discussion

3.1. Cell viability

The effects of NMs and MPLs on T98G and HeLa cells survival were evaluated using Hoechst 33258 as staining solution. Different concentrations between 50 μg/L and 10 mg/L of the selected NMs and MPLs in this work were studied individually. To obtain information regarding cell viability, the channel with 485 nm was selected in the HCA. However, no well-differentiated images were obtained for cells stained with Hoechst 33258 compared to those stained with DHE, as can be seen in Fig. S3 in Supporting Information. The main results of the cell viability study showed that none of the NMs or MPLs studied here did lead to a significant reduction of cell viability, as shown in Fig. 1. Therefore, cytolysis was not produced.

3.2. Oxidative stress of nanomaterials

A cytotoxic assay using DHE as staining solution was used to obtain information about the oxidative stress of selected NMs and MPLs on T98G and HeLa cell lines after 24 h of exposure.

As can be seen in Fig. 2A, in general, dose-dependent effects were obtained, with the exception of fullerol and ZrO_2-NPs in T98G cultured cells. In the case of fullerol, formation of aggregates drove the limitation of ROS production. On the other hand, in the case of ZrO_2-NPs, these were the biggest metal dioxide NPs studied here, and when the concentrations were over 0.5 mg/L, they tended to aggregate, and the ROS effects were modulated. Meanwhile, the greatest effects for T98G cells were produced by fullerene soot followed by TiO_2-NPs. It is noteworthy that cytotoxicity is highly influenced by the size and shape of NMs. For cytotoxicity comparison purposes, the particular characteristics of assayed NMs should be considered. The cells uptake biomolecules through endocytosis or can involve and entrap them by clathrin or caveolin pits or some proteins, and cell uptake and sub cellular distribution depend on their size (Shang et al., 2014). In addition, the medium can influence the size of NPs because of a change of ionic strength (Wyrwoll et al., 2016). In this study, the maximum of ROS production was shown to be limited by the aggregates generation in the

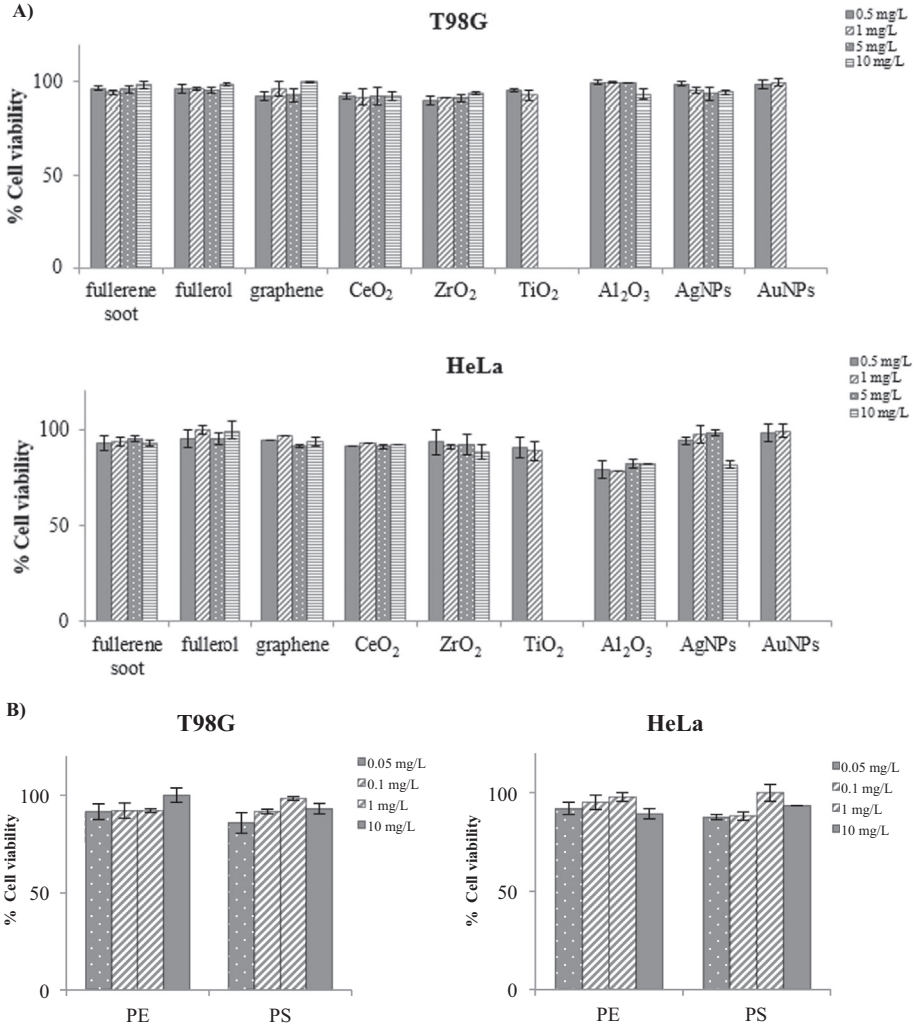

Fig. 1. Data obtained from HCA assay for metal oxide NPs, metal NPs, carbon NMs (A) and microplastics MPLs (B) on cerebral (T98G) and epithelial (HeLa) human cells. Data represented as live cells content. The *y*-axis represents the percentage of cell viability compared to the control. The *x*-axis represents the compounds used in the assay after a time period of 24 h of incubation. The different colors of the bars identify the concentration of the compounds. The values represent the mean ± standard deviation (SD) of three experiments.

cases of Fullerol and ZrO_2-NPs. However, the aggregation was previously characterized by NTA and in was shown stable during exposure, as in previous works. For example, Guadagnini et al., showed that the size of NPs in the cellular medium normally do not change at least 1 day, indicating the feasibility of in vitro testing without influence from potential agglomeration (Guadagnini et al., 2015).

Graphene is a two-dimensional layer of sp^2-hybridised carbon atoms. In previous studies, pristine graphene has been found to increase ROS and apoptosis. For example, in murine RAW 264.7 macrophages, the depletion of mitochondrial membrane potential (MMP) and ROS-triggered apoptosis was produced by the activation of the mitochondrial pathway (Li et al., 2012; Sasidharan et al., 2012). In another work, the potential influence of graphene on cell morphology, mortality, membrane integrity and cell viability was studied using the human glioblasoma U87 and U118 cells. In this study, it was found that graphene sheets had a strong tendency to localize close to the cells, but not enter inside the cells (Jaworski et al., 2013). However, in our findings, the exposure of cultured T98G and HeLa cells to fullerene soot led to an increase of intracellular reactive oxygen species only in HeLa cells and this effect was not very pronounced. It is noteworthy that previous studies showing a stronger ROS effects used, in general, graphene flakes composed of around 10 layers, and here we have used flakes composed of 30–50 layers. Both types of graphene are currently on the market, however, their effects are highly influenced by their particular characteristics. In addition, as already noted the most obvious difference between T98G cells and HeLa, which can induce DNA synthesis in senescent nuclei, is that T98G cells exhibit normal G1 growth regulation, whereas HeLa cells do not. We assume that this factor can influence on the major ROS response in HeLa cells.

While the graphene assayed here produced only effects at concentrations higher of 5 mg/L in HeLa cells, the results were contrary in the case of fullerol and fullerene soot, producing effects only on T98G cells. Fullerene soot was the NM producing the greatest effect on T98G cells in this study, while in HeLa cells no effects were observed.

In HeLa culture cells, major effects were produced byTiO_2-NPs followed by ZrO_2-NPs. In general, cytotoxicity of the metal oxide NPs depended on the particle composition and their uptake. Consequently, their incorporation into the cell could alter the membrane properties due to the generation of the ROS. The subcellular location in endosomal and caveolae compartments, or the lysosomes accumulation, could generate several effects such as organelle clumping, oxidative cell injury, mitochondrial depolarisation, cytokine release and cytotoxicity (Zbyszewski et al., 2014). Consequently, membrane fluidity decreases with relative modification of membrane-bound proteins and other radical species could also be generated (Cabiscol et al., 2010). Serum proteins and lipids present in the cellular medium improve NP dispersion or solution (Sager et al., 2007). In fact, the change from aqueous medium (PBS) to cellular medium (DMEM) during the standard preparation may influence NP size and consequently intracellular diffusion.

We have observed that TiO_2-NPs have induced ROS generation in both cell lines. Moreover, it was the NMs producing higher effects in HeLa cells. Previous studies on TiO_2-NPs toxicity provided conflicting results. The toxic effects have been reported by several studies, for

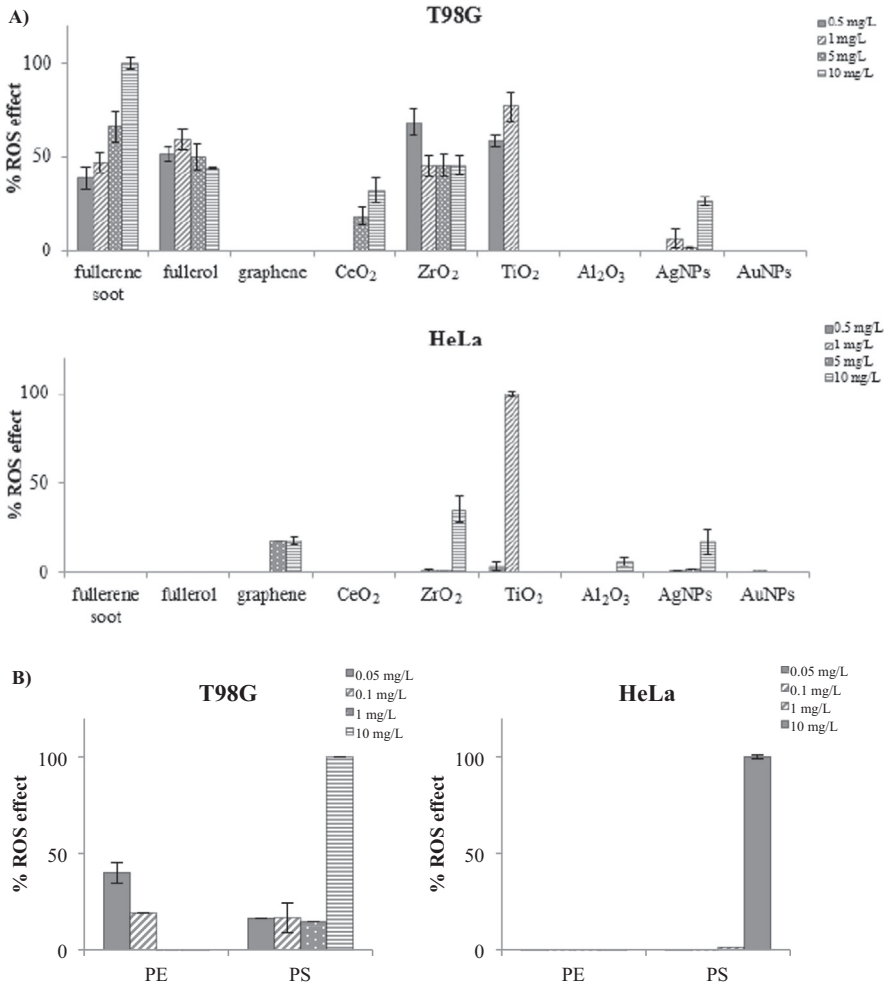

Fig. 2. Data obtained from HCA assay for metal oxide NPs, metal NPs, carbon NMs (A) and microplastics MPLs (B) on cerebral (T98G) and epithelial (HeLa) human cells. Data represented as Reactive Oxygen Species (ROS) effect. The *y* axis represents the percent ROS effect compared to the maximum effect observed after a time period of 24 h of exposure. The *x*-axis represents the compounds used in the HCA assay. The different colors of the bars identify the concentration of the compounds. The values represent the mean ± standard deviation of three experiments.

example, anatase TiO_2 nanoparticles were found to induced oxidative DNA damage, lipid peroxidation, micronuclei formation in a human bronchial epithelial cell line, in the absence of photo-activation (Gurr et al., 2005). Conversely, TiO_2-NPs in dark conditions were found not cytotoxic and not causing ROS generation in different studies (Hou et al., 2015; Tong et al., 2017; Zhang et al., 2014). For both type of results, it should be mentioned that the concentrations were much higher than those employed in the present study. In summary, cytotoxicity and oxidative stress of TiO_2 nanoparticles have been shown dependent on physicochemical properties as their structure or photocatalytic potency (Park et al., 2011). However, the concentration and aggregation could also be a modulation factor. In the present work, the maximum of ROS generation was obtained at 1 mg/L, and at higher concentrations, the ROS generation was not observed. This behaviour, observed in both cell lines, could be explained by the possibility of aggregates formation and the consequent depletion of cellular uptake at higher concentrations in dark conditions. The increase of ROS generation has been observed in several studies, under UV irradiation because of the photo-catalytic potential of TiO_2-NP, but also, probably, because the number of individual excited NPs able to be up-taken is increased by UV radiation. For example, Park et al. (2011) compared the cellular effects of TiO_2-NP with different photo-catalytic potential in human keratinocyte, HaCaT cells (Park et al., 2011) at concentrations from 50 to 150 mg/L, and much higher values of ROS effect was encountered after UV-irradiation. Consistent with these results, are the reported effects by irradiated TiO_2-NPs in HeLa cells by Zhang et al., but also with more recent studies on toxicity and ROS generation by irradiated TiO_2-NPs (Lu et al., 2017; Tong et al., 2017; Wang et al., 2014; Yamada et al., 2016). Therefore, the present finding can complement previous the information and underpinned the need to assess the effects at environmental concentrations since the behaviour of NPs is very much influenced by their aggregation and in general is not directly proportional to concentration.

Regarding metal NPs, at the highest concentration (1 mg/L) of AgNPs, ROS generation was increased in both cell lines. The toxicity of AgNPs is related to their surface charge (El Badawy et al., 2011), which varies according to the type and medium used during their synthesis. In this study, AgNPs were coated by the citrate functional group, which gives a negative surface charge. Therefore, citrate-AgNPs were repelled by the negative charge of cellular membranes. However, once the electrostatic barrier is overcome, at high concentrations of NPs, NPs can penetrate cellular membranes and interact physically or chemically with the mitochondria, resulting in oxidative stress. Cytotoxicity of NPs can be an effect of alteration of mitochondrial function, expressly with an uncoupling oxidation of the phosphorylation membrane system.

However, there was no significant variation in T98G neither in HeLa cells exposed to AuNPs, which is in agreement with previous studies with different cell lines (Austin et al., 2015; Ristig et al., 2015; Connor et al., 2005). With respect to general trends, the ROS generation in both cell lines followed a different trend.

It is noteworthy that at the low concentrations assayed (low in comparison to those that are, in general, studied for the use of NPs in nanomedicine), a different picture was obtained. For example, in the case of AgNPs, strong effects are, in general, reported as being obtained at higher concentrations, while in the case of carbon NMs the association of aggregates inhibits their bioavailability.

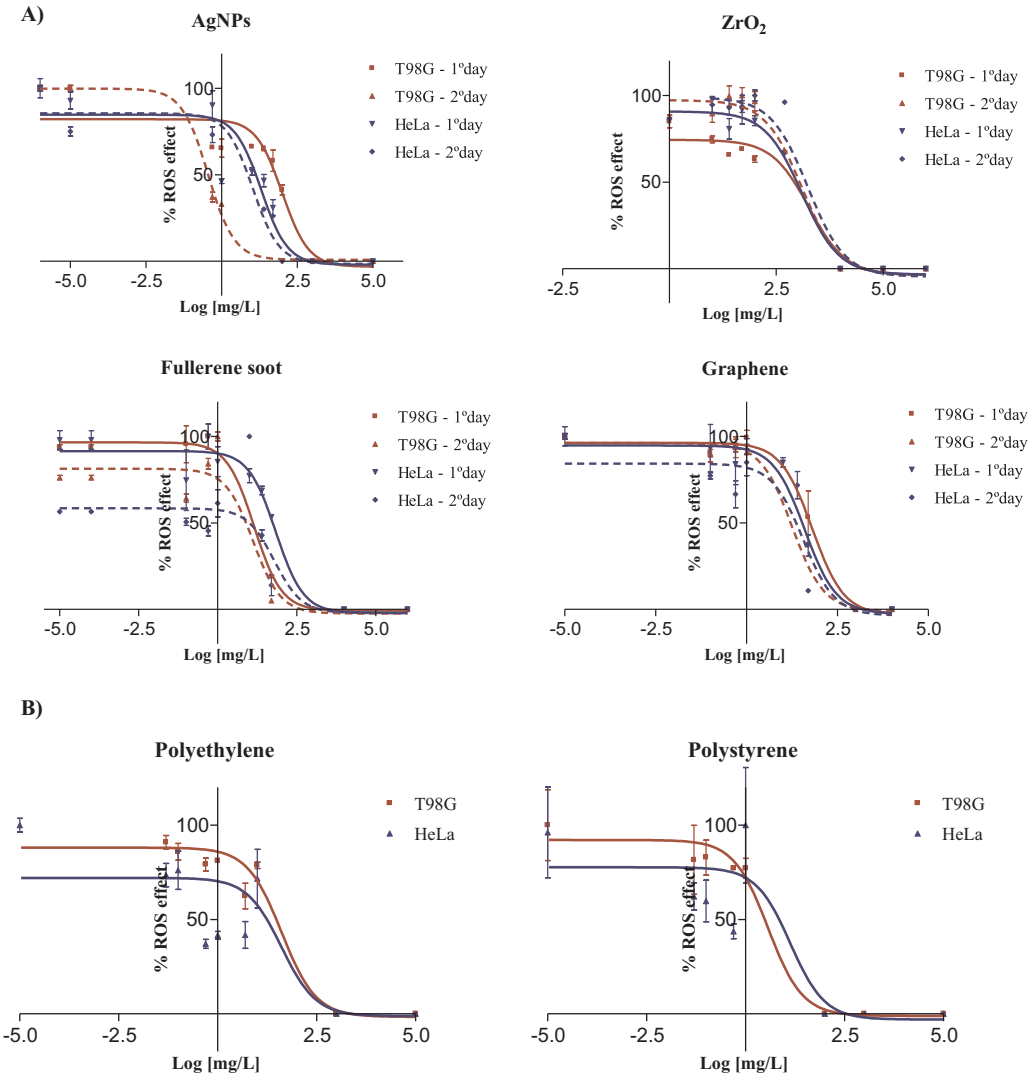

Fig. 3. Dose response curve showing the ROS effect (%) of T98G and HeLa cell lines exposed for 48 h to increasing doses of metal oxide NPs, metal NPs, carbon NMs (A). Dose response curve showing the ROS effect (%) of T98G and HeLa cell lines exposed for a time period of 24 h to increasing doses of microplastics (B). The data presented are the mean ± SD of three independent experiments.

Table 1
EC_{50} values for the exposure of AgNPs, ZrO_2, graphene and fullerene soot to cerebral (T98G) and epithelial (HeLa) human cells for 72 h, as determined by HCA assay.

Compounds	**EC_{50} (mg/L)** (95% confidence intervals)			
	T98G		**HeLa**	
	1° day	*2° day*	*1° day*	*2° day*
AgNPs	101.5 (54.9–187.6)	0.4 (0.3–0.5)	20.4 (9.9–41)	10.8 (4.1–29)
ZrO_2	1831 (938.7 – 3572)	1265 (398.4 – 3824)	1257 (711.9 – 2221)	1730 (791.9 – 3781)
Graphene	64.56 (35.7–116.7)	18.13 (17 – 193.2)	39.92 (20.4–78)	36.36 (15.7–84.1)
Fullerene soot	14.16 (6.7–29.8)	13.13 (2.5–40)	68.76 (33.9–139.4)	61.60 (20.5–185.3)

As second step, both cells lines were exposed for 48 h to the contaminants that showed a more notorious cytotoxic effect, such as AgNPs, ZrO_2, graphene, and fullerene soot. Moreover, the maximum concentration assayed was at least 10 times greater. The dose response curves were fitted (Fig. 3) and the half maximal effective concentrations (EC_{50}) were calculated (Table 1). As can be shown in T98G cells, in the two periods of exposure, fullerene soot presented the lower EC_{50} but the maximum effect was at the 60%. This indicates that over a concentration the hydrophobicity of fullerenes drives to auto-aggregation limiting their ROS generation. While, in the case of AgNPs ROS generation is slowly produced.

It should be highlighted that we have studied the potential effects at concentrations that can be the result of bioaccumulation from the environment. Therefore, higher than environmental reported or estimated concentrations and much lower than concentrations previously explored when the potential toxicity of NMs for it use as drug carriers was studied, in occupational exposure studies, or when what is explore it's the elucidation of the general mode of action.

Table 2
EC_{50} values for the exposure of polyethylene and polystyrene to cerebral (T98G) and epithelial (HeLa) human cells for 24 h, as determined by HCA assay.

	EC_{50} (mg/L) (95% confidence intervals)	
Compounds	**T98G**	**HeLa**
Polyethylene	41.22 (12.8–133)	40.96 (17.8–178.8)
Polystyrene	9.617 (3.9–23.8)	13.56 (2–96)

3.3. Oxidative stress of microplastics

In the case of PE, ROS generation was only significant on T98G. However in both cell cultures PS presented a higher ROS generation. Probably, this effect can be related to the smaller size of PS particles (Fig. 2 B, Table 2). After control substraction, no significant ROS generation was observed in some cases when cells were exposed to PE.

3.3.1. Trojan Horse effect

The synergistic and antagonistic relationships between fullerenes and three selected organic contaminants (malathion, C12-LAS and DEHP) were assessed. The ROS generation of a range of different nominal concentrations of these contaminants (malathion between 5 and 30 mg/L; C12-LAS between 5 and 50 mg/L and DEHP between 0.5 and 50 mg/L) was assessed with and without fullerenes. In the mixtures with fullerene soot, two concentrations (1 and 5 mg/L) were tested. The experimental results were compared with the theoretical values according to a simple additive model.

As can be seen in Fig. 4, in the case of malathion, this compound has been related to ROS generation at concentrations around 40 mg/L in PC12 cells. In our study using T98G cell, also almost no ROS generation (around 5%) was observed for concentrations of exposure inferior to 30 mg/L. Therefore, according to a simple additive model, the ROS generation in this mixture should be attributed mainly to fullerenes.

Due to the hydrophobicity of malathion (log Kow = 2.7 at 25 °C), in a first step fullerene soot will adsorb malathion and tend to be deposited onto the membrane cells. When fullerene soot concentrations were high enough, malathion was efficiently retained and probably assisted in the formation of bigger fullerene aggregates. This can contribute to decreasing the bioavailability in agreement with the observed antagonistic effect. Whereas, in those binary mixtures where fullerene aggregates surface was saturated, loosely attached malathion molecules were released directly on membranes surface and the synergistic effect was then produced. The same behaviour was observed in the case of *D. magna* exposed to mixtures of malathion and fullerene soot (Sanchís et al., 2015).

A similar behaviour was observed in the case of C12-LAS. This surfactant alone did not present ROS generation on T98g cells. Again, ideally, the ROS generation of the mixture should be only the contribution of fullerene soot following a simple additive model. However, for the lower concentrations of C12-LAS between 5 and 25 mg/L we have observed antagonism. And, this effect was clearly more pronounced when the ratio between fullerene soot and C2-LAS was higher. In a first step, fullerenes are sequestering C12-LAS from solution and when fullerene soot concentrations were high enough, C12-LAS was efficiently retained. The surfactant character of C12-LAS contributes again to the formation of hetero-aggregates contributing to the bioavailability decrease. However, in one case, when the concentration of fullerenes was 50 mg/L and the concentration of fullerene soot was 1 mg/L, synergism was produced. In this case, fullerenes surface was saturated, free C12-LAS surfactants did not reach their critical micelle concentration (100 mg/L) for auto-aggregation and, therefore, tended to be associated to membrane cells and membrane solubilisation. Notwithstanding, for the same concentration of C12-LAS, but with 10 times more fullerene soot, then C12- is attached to fullerene surface, hetero-aggregates are favored, bioavailability is decreased and an antagonistic effect was observed.

Finally, DEHP presented ROS generation that was directly proportional with concentration. Once again, DEHP molecules tended to be adsorbed on the fullerene aggregate surface and hetero-aggregates and synergistic effects were shown. Only when concentrations of DEHP were high enough was 100% of effect reached, as expected.

These results are a pioneer observation of the Trojan-Horse mechanism at cell level and they underpin the necessity of assessing the presence and effect of carbon nanomaterials in the marine environment, since they are active agents, which are changing the bioavailability of xenobiotics.

4. Conclusions

HCA has proven to be a powerful, robust, reliable technique for the simultaneous observation and toxicity assessment of cells exposed to nanoparticles and common organic contaminants, and it has allowed assessment of the toxic effects of nanomaterials and two types of microplastics of two different types of cell. The data provided in this work complement previous studies conducted and much higher concentrations, which is important since toxicity of NPs is not always dose-dependent. Also, these results are focussed on potential toxicity produced by bioaccumulation in the environment offering data relevant for posterior risk–assessment studies evaluating the risks for human health. For example, considering that it has been widely reported that ROS generation had a critical role in the growth and proliferation of cancer cells (Tang et al., 2011; Manda et al., 2015; Poillet-Perez et al., 2015). During the recent years, the use of in vitro approaches has to gain interest for assessing the risks of chemicals and drugs in a more mechanistic and high throughput manner than in vivo tests. Different models have been developed in recent years for the quantitative in-vitro to in-vivo toxicity assays, in particular, in the case of cell-lines. Physiologically based pharmacokinetic (PBPK) modelling provides a practical framework for conducting quantitative in vitro to in vivo extrapolation (Yoon et al., 2012; Wetmore, 2015).

The obtained results contribute to the current knowledge of the cytotoxcity of both nanomaterials and microplastics, whereby oxidative stress is one mechanism that explains the toxicity of these emerging contaminants at cell level, as has been observed for both T98G and HeLa lines.

In addition, carbon nanomaterials have the potential to interact in a complex way with the co-occurring contaminants, changing the bioavailability and, therefore, their resulting toxicity in either a synergistic or an antagonistic way. The result of this study showed that fullerene soot presented a predominantly antagonistic effect in binary mixtures with other organic contaminants. To the best of knowledge, this fact agrees with previous results obtained in ecotoxicological studies.

In general, these phenomena have been overlooked during risk assessments of these substances and more attention should be paid to them in the future. Other nano-structured materials, such as nano-sized plastics or metal-oxide nanoparticles, may modulate the toxicity of co-contaminants (Sanchís et al., 2015). In the same manner, recent studies (Vidali et al., 2016) provide evidence that the toxic behaviour of NMs such as carbon nanotubes could be altered with unknown effects on humans, and the environment by environmental factors and these topics must be further studied.

Acknowledgements

This work was funded by Integra-Coast (CGL2014-56530-C4-1-R). The authors would like to express their deepest gratitude to IQAC-CSIC with respect to their work contribution during the cell culture. We also express our gratitude towards Thermo Fisher Scientific with reference

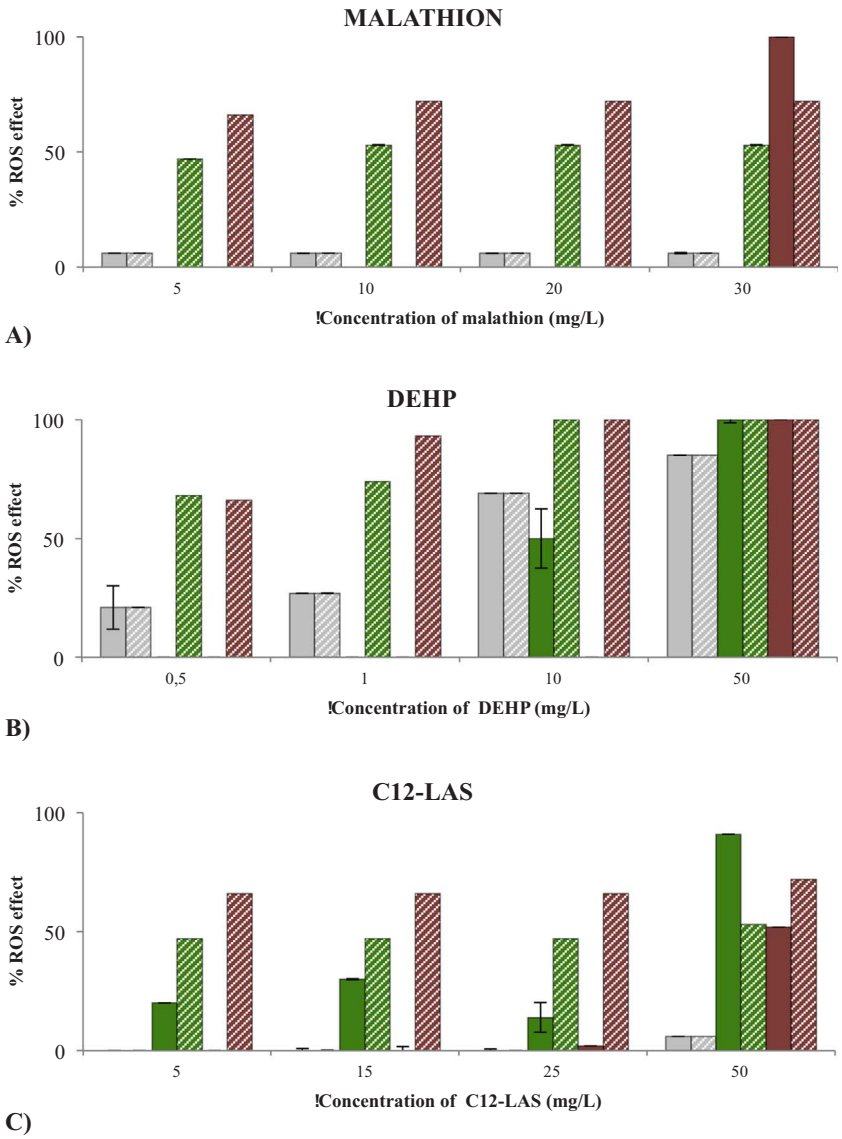

Fig. 4. Data obtained from HCA assay for binary mixture of fullerenes soot and organic compounds such as malathion (A), DEHP (B) and C12-LAS (C) on the cerebral human cells (T98G). Data represented as Reactive Oxygen Species (ROS) effect. The *y*-axis represents the percent ROS effect compared to the maxim effect observed after 24 h of time of exposure. The *x*-axis represents the concentration of fullerenes soot in the binary mixture. The different colors of the bars identify the concentration of the compounds. The values represent the mean ± standard deviation of three experiments.

to Thermo Scientific CellInsight™ NXT High Content Screening (HCS) Platform.

Appendix A. Supporting information

Supplementary data associated with this article can be found in the online version at http://dx.doi.org/10.1016/j.envres.2017.08.043.

References

Al-Salem, S.M., Lettieri, P., Baeyens, J., 2010. The valorization of plastic solid waste (PSW) by primary to quaternary routes: from re-use to energy and chemicals. Progr. Energy Combust. Sci. 36, 103–129.

Aueviriyavit, Sasitorn, Phummiratch, Duangkamol, Maniratanachote, Rawiwan, 2014. Mechanistic study on the biological effects of silver and gold nanoparticles in Caco-2 cells – Induction of the Nrf2/HO-1 pathway by high concentrations of silver nanoparticles. Toxicol. Lett. 224, 73–83.

Austin, Lauren A., Ahmad, Samera, Kang, Bin, Rommel, Kathryn R., Mahmoud, Mahmoud, Peek, Mary E., El-Sayed, Mostafa A., 2015. Cytotoxic effects of cytoplasmic-targeted and nuclear-targeted gold and silver nanoparticles in HSC-3 cells – A mechanistic study. Toxicol. In Vitro 29, 694–705.

Cabiscol, Elisa, Tamarit, Jordi, Ros, Joaquim, 2010. Oxidative stress in bacteria and protein damage by reactive oxygen species. Int. Microbiol. 3, 3–8.

Cedervall, Tommy, Hansson, Lars-Anders, Lard, Mercy, Frohm, Birgitta, Linse, Sara, 2012. Food chain transport of nanoparticles affects behaviour and fat metabolism in fish. PLoS One 7, e32254.

Cole, Matthew, Lindeque, Pennie, Halsband, Claudia, Galloway, Tamara S., 2011. Microplastics as contaminants in the marine environment: a review. Mar. Pollut. Bull. 62, 2588–2597.

Connor, Ellen E., Mwamuka, Judith, Gole, Anand, Murphy, Catherine J., Wyatt, Michael D., 2005. Gold nanoparticles are taken up by human cells but do not cause acute cytotoxicity. Small 1, 325–327.

Contado, C., 2015. Nanomaterials in consumer products: a challenging analytical problem. Front. Chem. 3.

da Costa, J.P., Duarte, A.C., Rocha-Santos, T.A.P., 2017. Microplastics - Occurrence, Fate and Behaviour in the Environment. In Comprehensive Analytical Chemistry.

Dykman, Lev, Khlebtsov, Nikolai, 2012. 'Gold nanoparticles in biomedical applications: recent advances and perspectives'. Chem. Soc. Rev. 41, 2256–2282.
El Badawy, Amro M., Rendahandi, G. Silva, Morris, Brian, Scheckel, Kirk G., Suidan, Makram T., Tolaymat, Thabet M., 2011. Surface charge-dependent toxicity of silver nanoparticles. Environ. Sci. Technol. 45, 283–287.
Eleftheriadou, M., Pyrgiotakis, G., Demokritou, P., 2017. 'Nanotechnology to the rescue: using nano-enabled approaches in microbiological food safety and quality'. Curr. Opin. Biotechnol. 44, 87–93.
Farré, M., Barceló, D., 2012. Introduction to the analysis and risk of nanomaterials in environmental and food samples. In Comprehensive Analytical Chemistry, 1–32.
Lee, Hyang Yeon, Park, Hyoung Kun, Lee, Yoon Mi, Kim, Kwan, Park, Seung Bum, 2007. A practical procedure for producing silver nanocoated fabric and its antibacterial evaluation for biomedical applications. Chem. Commun. 2959–2961.
Fendall, Lisa S., Mary, A. Sewell, 2009. Contributing to marine pollution by washing your face: microplastics in facial cleansers. Mar. Pollut. Bull. 58, 1225–1228.
Fu, Peter P., Xia, Qingsu, Hwang, Huey-Min, Ray, Paresh C., Yu, Hongtao, 2014. Mechanisms of nanotoxicity: generation of reactive oxygen species. J. Food Drug Anal. 22, 64–75.
Guadagnini, Rina, Kenzaoui, Blanka Halamoda, Walker, Laura, Pojana, Giulio, Magdolenova, Zuzana, Bilanicova, Dagmar, Saunders, Margaret, Juillerat-Jeanneret, Lucienne, Marcomini, Antonio, Huk, Anna, 2015. Toxicity screenings of nanomaterials: challenges due to interference with assay processes and components of classic in vitro tests. Nanotoxicology 9, 13–24.
Gurr, J.R., Wang, A.S.S., Chen, C.H., Jan, K.Y., 2005. Ultrafine titanium dioxide particles in the absence of photoactivation can induce oxidative damage to human bronchial epithelial cells. Toxicology 213, 66–73.
Holden, P.A., Gardea-Torresdey, J.L., Klaessig, F., Turco, R.F., Mortimer, M., Hund-Rinke, K., Cohen Hubal, E.A., Avery, D., Barceló, D., Behra, R., Cohen, Y., Deydier-Stephan, L., Ferguson, P.L., Fernandes, T.F., Herr Harthorn, B., Henderson, W.M., Hoke, R.A., Hristozov, D., Johnston, J.M., Kane, A.B., Kapustka, L., Keller, A.A., Lenihan, H.S., Lovell, W., Murphy, C.J., Nisbet, R.M., Petersen, E.J., Salinas, E.R., Scheringer, M., Sharma, M., Speed, D.E., Sultan, Y., Westerhoff, P., White, J.C., Wiesner, M.R., Wong, E.M., Xing, B., Horan, M. Steele, Godwin, H.A., Nel, A.E., 2016. Considerations of environmentally relevant test conditions for improved evaluation of ecological hazards of engineered nanomaterials. Environ. Sci. Technol. 50, 6124–6145.
Horton, A.A., Walton, A., Spurgeon, D.J., Lahive, E., Svendsen, C., 2016. Microplastics in freshwater and terrestrial environments: evaluating the current understanding to identify the knowledge gaps and future research priorities. Sci. Total Environ.
Hou, Z., Zhang, Y., Deng, K., Chen, Y., Li, X., Deng, X., Cheng, Z., Lian, H., Li, C., Lin, J., 2015. UV-emitting upconversion-based TiO < inf > 2 < /inf > photosensitizing nanoplatform: near-infrared light mediated in vivo photodynamic therapy via mitochondria-involved apoptosis pathway. ACS Nano 9, 2584–2599.
Jaworski, S., Sawosz, E., Grodzik, M., Winnicka, A., Prasek, M., Wierzbicki, M., Chwalibog, A., 2013. In vitro evaluation of the effects of graphene platelets on glioblastoma multiforme cells. Int. J. Nanomed. 8, 413–420.
Johnston, Helinor J., Hutchison, Gary, Christensen, Frans M., Peters, Sheona, Hankin, Steve, Stone, Vicki, 2010. A review of the in vivo and in vitro toxicity of silver and gold particulates: particle attributes and biological mechanisms responsible for the observed toxicity. Crit. Rev. Toxicol. 40, 328–346.
Khanna, Puja, Ong, Cynthia, Bay, Boon, Baeg, Gyeong, 2015. Nanotoxicity: an interplay of oxidative stress, inflammation and cell death. Nanomaterials 5, 1163.
Kratschmer, W., Lowell, D. Lamb, Fostiropoulos, K., Huffman, Donald R., 1990. Solid C60: a new form of carbon. Nature 347, 354–358.
Li, Y., Liu, Y., Fu, Y., Wei, T., Le Guyader, L., Gao, G., Liu, R.S., Chang, Y.Z., Chen, C., 2012. The triggering of apoptosis in macrophages by pristine graphene through the MAPK and TGF-beta signaling pathways. Biomaterials 33, 402–411.
Llorca, Marta, Farré, Marinella, Karapanagioti, Hrissi K., Barceló, Damià, 2014. Levels and fate of perfluoroalkyl substances in beached plastic pellets and sediments collected from Greece. Mar. Pollut. Bull. 87, 286–291.
Lu, H., Fan, W., Dong, H., Liu, L., 2017. 'Dependence of the irradiation conditions and crystalline phases of TiO < inf > 2 < /inf > nanoparticles on their toxicity to Daphnia magna. Environ. Sci.: Nano 4, 406–414.
Maes, Hanna M., Stibany, Felix, Giefers, Sebastian, Daniels, Benjamin, Deutschmann, Björn, Baumgartner, Werner, Schäffer, Andreas, 2014. Accumulation and distribution of multiwalled carbon nanotubes in zebrafish (Danio rerio). Environ. Sci. Technol. 48, 12256–12264.
Manda, G., Isvoranu, G., Comanescu, M.V., Manea, A., Debelec Butuner, B., Korkmaz, K.S., 2015. The redox biology network in cancer pathophysiology and therapeutics. Redox Biol. 5, 347–357.
Marchesan, S., Prato, M., 2013. Nanomaterials for (Nano)medicine. ACS Med. Chem. Lett. 4, 147–149.
Nickel, Carmen, Angelstorf, Judith, Bienert, Ralf, Burkart, Corinna, Gabsch, Stephan, Giebner, Sabrina, Haase, Andrea, Hellack, Bryan, Hollert, Henner, Hund-Rinke, Kerstin, Jungmann, Dirk, Kaminski, Heinz, Luch, Andreas, Maes, Hanna M., Nogowski, André, Oetken, Matthias, Schaeffer, Andreas, Schiwy, Andreas, Schlich, Karsten, Stintz, Michael, Kammer, Frank von der, Kuhlbusch, Thomas A.J., 2014. Dynamic light-scattering measurement comparability of nanomaterial suspensions. J. Nanopart. Res. 16, 2260.
Park, H.O., Yu, M., Kang, S.K., Yang, S.I., Kim, Y.J., 2011. Comparison of cellular effects of titanium dioxide nanoparticles with different photocatalytic potential in human keratinocyte, HaCaT cells. Mol. Cell. Toxicol. 7, 67–75.
Poillet-Perez, L., Despouy, G., Delage-Mourroux, R., Boyer-Guittaut, M., 2015. Interplay between ROS and autophagy in cancer cells, from tumor initiation to cancer therapy. Redox Biol. 4, 184–192.
Ranjan, S., Dasgupta, N., Chakraborty, A.R., Melvin Samuel, S., Ramalingam, C., Shanker, R., Kumar, A., 2014. Nanoscience and nanotechnologies in food industries: opportunities and research trends. J. Nanopart. Res. 16.
Rashid, Mamun Ur, Hassan Bhuiyan, Md. Khairul, Quayum, M. Emran, 2013. Synthesis of silver nano particles (Ag-NPs) and their uses for quantitative analysis of vitamin C tablets. Dhaka Univ. J. Pharm. Sci. 12, 29–33.
Rico, Cyren M., Majumdar, Sanghamitra, Duarte-Gardea, Maria, Peralta-Videa, Jose R., Gardea-Torresdey, Jorge L., 2011. Interaction of nanoparticles with edible plants and their possible implications in the food chain. J. Agric. Food Chem. 59, 3485–3498.
Ristig, Simon, Chernousova, Svitlana, Meyer-Zaika, Wolfgang, Epple, Matthias, 2015. Synthesis, characterization and in vitro effects of 7 nm alloyed silver–gold nanoparticles. Beilstein J. Nanotechnol. 6, 1212–1220.
Sager, Tina M., Dale, W. Porter, Robinson, Victor A., Lindsley, William G., Schwegler-Berry, Diane E., Castranova, Vincent, 2007. Improved method to disperse nanoparticles for in vitro and in vivo investigation of toxicity. Nanotoxicology 1, 118–129.
Sanchez, C., Belleville, P., Popall, M., Nicole, L., 2011. Applications of advanced hybrid organic-inorganic nanomaterials: from laboratory to market. Chem. Soc. Rev. 40, 696–753.
Sanchís, J., Olmos, M., Vincent, P., Farré, M., Barceló, D., 2016. New insights on the influence of organic co-contaminants on the aquatic toxicology of carbon nanomaterials. Environ. Sci. Technol. 50, 961–969.
Sanchís, Josep, Olmos, Mar, Vincent, Phil, Farre, Marinella, Damià, Barceló, 2015. New insights on the influence of organic co-contaminants on the aquatic toxicology of carbon nanomaterials. Environ. Sci. Technol. 50, 961—9669.
Sasidharan, A., Panchakarla, L.S., Sadanandan, A.R., Ashokan, A., Chandran, P., Girish, C.M., Menon, D., Nair, S.V., Rao, C.N.R., Koyakutty, M., 2012. Hemocompatibility and macrophage response of pristine and functionalized graphene. Small 8, 1251–1263.
Shang, Li, Nienhaus, Karin, Nienhaus, Gerd Ulrich, 2014. Engineered nanoparticles interacting with cells: size matters. J. Nanobiotechnol. 12, 5.
Tang, H., Qin, Y., Li, J., Gong, X., 2011. The scavenging of superoxide radicals promotes apoptosis induced by a novel cell-permeable fusion protein, sTRAIL: FeSOD, in tumor necrosis factor-related apoptosis-inducing ligand-resistant leukemia cells. BMC Biol. 9.
Tong, R., Lin, H., Chen, Y., An, N., Wang, G., Pan, X., Qu, F., 2017. Near-infrared mediated chemo/photodynamic synergistic therapy with DOX-UCNPs@ mSiO < inf > 2 < /inf > /TiO < inf > 2 < /inf > -TC nanocomposite. Mater. Sci. Eng. C 78, 998–1005.
Tongesayi, S., Tongesayi, T. 2016. Water Quality and Public Health: Role of Wastewater. in, Chemistry and Water: The Science Behind Sustaining the World's Most Crucial Resource.
Vidali, M.S., Bletsa, E., Kouloumpis, A., Skoutelis, C.G., Deligiannakis, Y., Gournis, D., Vlastos, D., 2016. Induction of micronuclei by multi-walled carbon nanotubes interacting with humic acids in cultured human lymphocytes. Environ. Sci.: Nano 3, 74–84.
Vigneshwaran, N., Kathe, A.A., Varadarajan, P.V., Nachane, R.P., Balasubramanya, R.H., 2007. Functional finishing of cotton fabrics using silver nanoparticles. J. Nanosci. Nanotechnol. 7, 1893–1897.
Wang, D., Zhao, L., Guo, L.H., Zhang, H., 2014. Online detection of reactive oxygen species in ultraviolet (UV)-irradiated nano-TiO < inf > 2 < /inf > suspensions by continuous flow chemiluminescence. Anal. Chem. 86, 10535–10539.
Wetmore, Barbara A., 2015. Quantitative in vitro-to-in vivo extrapolation in a high-throughput environment. Toxicology 332, 94–101.
Wijnhoven, Susan W.P., Willie, J.G.M. Peijnenburg, Herberts, Carla A., Hagens, Werner I., Agnes, G. Oomen, Evelyn, H.W. Heugens, Roszek, Boris, Bisschops, Julia, Gosens, Ilse, De Meent, Dik Van, 2009. Nano-silver–a review of available data and knowledge gaps in human and environmental risk assessment. Nanotoxicology 3, 109–138.
Wright, Stephanie L., Thompson, Richard C., Galloway, Tamara S., 2013. The physical impacts of microplastics on marine organisms: a review. Environ. Pollut. 178, 483–492.
Wyrwoll, Anne J., Lautenschläger, Petra, Bach, Alexander, Hellack, Bryan, Dybowska, Agnieszka, Kuhlbusch, Thomas A.J., Hollert, Henner, Schäffer, Andreas, Maes, Hanna M., 2016. Size matters–the phototoxicity of TiO 2 nanomaterials. Environ. Pollut. 208, 859–867.
Yamada, I., Nomura, K., Iwahashi, H., Horie, M., 2016. The effect of titanium dioxide (TiO < inf > 2 < /inf >) nano-objects, and their aggregates and agglomerates greater than 100nm (NOAA) on microbes under UV irradiation. Chemosphere 143, 123–127.
Yan, Liang, Zhao, Feng, Li, Shoujian, Hu, Zhongbo, Zhao, Yuliang, 2011. Low-toxic and safe nanomaterials by surface-chemical design, carbon nanotubes, fullerenes, metallofullerenes, and graphenes. Nanoscale 3, 362–382.
Yoo-Iam, Maneekarn, Chaichana, Ratcha, Satapanajaru, Tunlawit, 2014. Toxicity, bioaccumulation and biomagnification of silver nanoparticles in green algae (Chlorella sp.), water flea (Moina macrocopa), blood worm (Chironomus spp.) and silver barb (Barbonymus gonionotus). Chem. Speciat. Bioavailab. 26, 257–265.
Yoon, Miyoung, Jerry, L. Campbell, Andersen, Melvin E., Clewell, Harvey J., 2012. Quantitative in vitro to in vivo extrapolation of cell-based toxicity assay results. Crit. Rev. Toxicol. 42, 633–652.
Zbyszewski, M., Corcoran, P.L., Hockin, A., 2014. Comparison of the distribution and degradation of plastic debris along shorelines of the Great Lakes, North America. J. Gt. Lakes Res. 40.
Zhang, S., Yang, D., Jing, D., Liu, H., Liu, L., Jia, Y., Gao, M., Guo, L., Huo, Z., 2014. Enhanced photodynamic therapy of mixed phase TiO2(B)/anatase nanofibers for killing of HeLa cells. Nano Res.